









(> 1160 nm, in the Fourier plane of the prism-compressor) of the continuum are blocked to record a background-free  $I_{FWM}$  which corresponds to the short wavelength part of the continuum (< 1160 nm). For the second measurement the short wavelength components (< 1060 nm) of the broadband continuum pulse are blocked to record the FWM signal which corresponds to the long wavelength part of the continuum (> 1060 nm). In this way the interaction between the wings of the continuum is inhibited. Combination of the two measurements yields the background-free XFROG trace (see Fig. 3). The acquired spectrogram contains the information about the laser pulse relative spectral intensity  $I_c(\omega)$  and group-delay  $t_{gd}$ . With the narrowband gate pulse at 776.7 nm the FWM signal reproduces the laser spectrum. Integrating along the time-axis  $\tau$  delivers the relative spectral intensity  $\propto \int_{-\infty}^{\infty} I_{XFROG}(\tau, \omega) d\tau$  from which the laser spectrum  $E_c(\omega)$  is determined by wavelength conversion (see Fig. 3(c)).

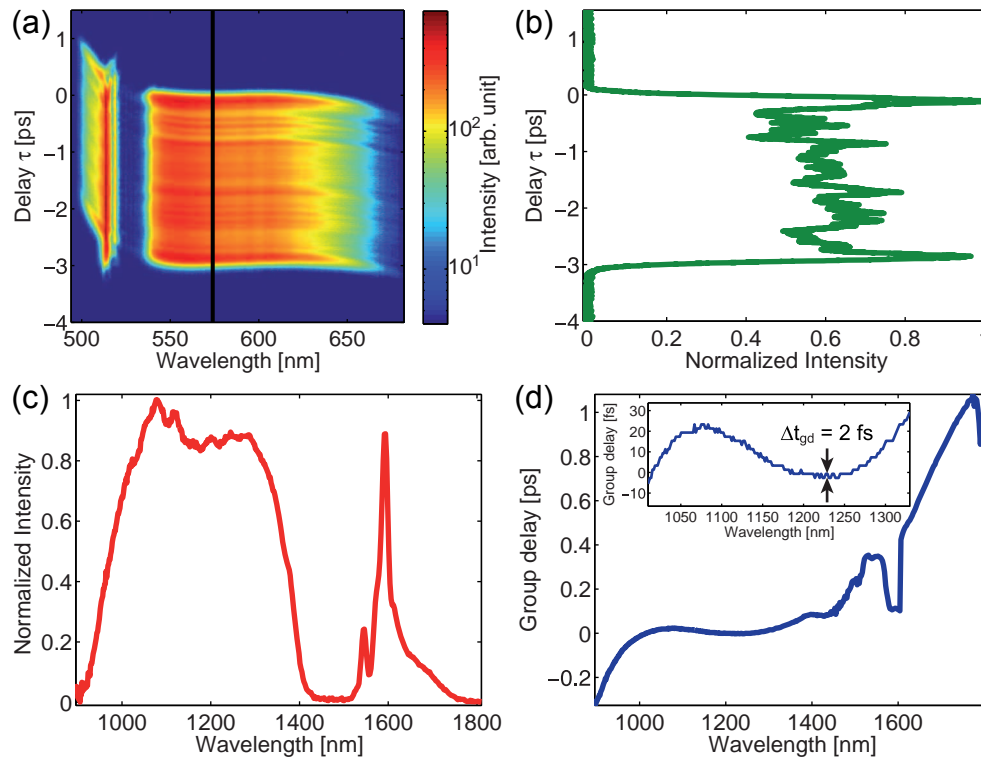


Fig. 3. (a) Measured XFROG spectrogram with a CCD camera exposure time of 1 ms and time delay steps of 2 fs, (b) Reference cross-correlation, section at 574 nm indicated by vertical line in (a) (corresponds to 1200 nm in the continuum), (c) Retrieved laser spectrum  $E_c(\omega)$  by averaging over time delay  $\tau$ , (d) Retrieved group delay  $t_{gd}$  with a zoomed inset which indicates a temporal error of 2 fs.

The group delay versus wavelength is directly observable in the contour of the spectrogram (see Fig. 3(a)). For group delay extraction a reference gate in the spectrogram at an arbitrary wavelength (here  $\lambda_{FWM} = 574$  nm, which corresponds to 1200 nm in the continuum) is chosen (see vertical line in Fig. 3(a)). The section is shown in Fig. 3(b) and corresponds to the squared intensity envelope of the gate pulse (compare Fig. 2). This temporal profile is reproduced at all wavelengths throughout the spectrogram but with a temporal shift which corresponds to the group delay of the continuum pulse. Tracking this reference shape along all wavelength positions of the FWM-XFROG spectrogram unveils the corresponding group delay. This result

is achieved by calculating the cross-correlation between the reference gate at 574 nm and the sections through the spectrogram along all wavelengths. Since the respective profiles have an overall rectangular shape, the cross-correlations are triangular and therefore their maximum is precisely defined. The temporal position of the maximum of the cross-correlations directly yields the group delay  $t_{gd}$ . Due to the steep slopes at the leading and trailing edge of the gate pulse, a good temporal resolution is obtained. In the inset of Fig. 3(d) a zoomed graph is shown which indicates a temporal error of 2 fs. One should note that a small error in the determination of  $t_{gd}$  has a relatively small effect on the determination of the pulse duration. Plugging  $t_{gd}$  in Eq. (3) leads to the spectral phase  $\phi(\omega)$ . In this way the electric field can be completely determined, except for a constant phase offset which is not relevant for the determination of the envelope. This finding shows that the characterization of complicated laser pulses is possible with our technique.

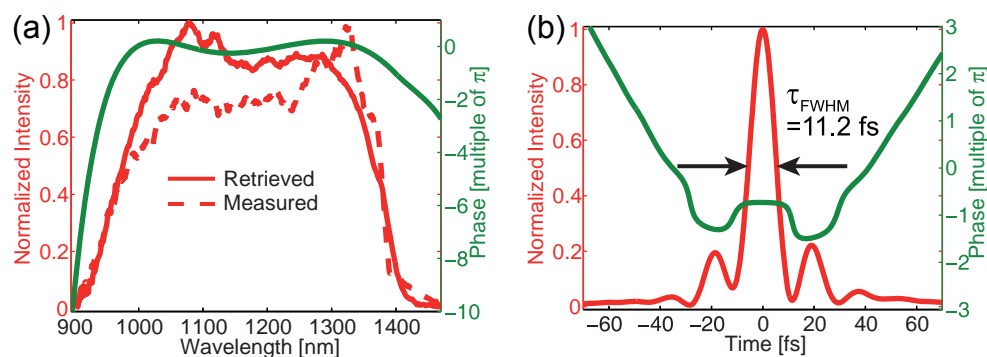


Fig. 4. (a) Retrieved intensity and phase spectra as well as the intensity spectrum measured by a linear spectrometer, (b) The retrieved temporal intensity envelope and phase show a pulse duration of 11.2 fs.

An analysis of the short wavelength part of the continuum is demonstrated by blocking the wavelength components above 1500 nm of the supercontinuum in the Fourier plane of the prism compressor (see Fig. 4(a)). Characterization of the compressed spectrum unveils a pulse duration of  $\tau_{FWHM}=11.2$  fs (bandwidth limit: 8.4 fs) in the focus of a microscope objective as well as the spectral phase information. Any linear phase function can be subtracted from the experimentally determined trace which affects the absolute time delay of the pulse envelope but not its shape. Therefore a linear phase is subtracted from the experimental phase for best visualization of the phase curvature (see Fig. 4(a)). Fourier transform yields the pulse intensity envelope as well as the phase in the time domain (see Fig. 4(b)). The validity of the XFROG scheme is verified by comparison of a calculated second-harmonic FRAC trace based on the XFROG retrieved electric field with an independent second-harmonic FRAC measurement. Although the FRAC technique shows some phase ambiguities it is never the less a frequently used pulse characterization technique and therefore we think suitable for our validation. A good agreement between the two traces is observable in Fig. 5. This result demonstrates the applicability of the technique for ultrashort laser pulses in the few cycle regime.

#### 4. Conclusion

The presented method allows for direct extraction of the group delay as a function of frequency of an octave spanning supercontinuum output of the highly nonlinear fiber enabled by the broad phase-matching bandwidth of the FWM process in the microscope focus. High temporal and spectral resolution is exploited by the flat-top shape of the gate pulse. Direct reconstruction

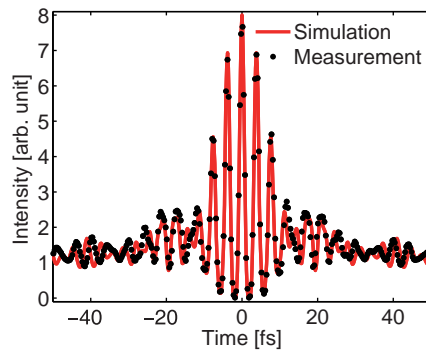


Fig. 5. Line: Calculated second-harmonic fringe-resolved autocorrelation based on the XFROG retrieved spectrum and phase, dots: Measured second-harmonic fringe-resolved autocorrelation.

of the electric field envelope is demonstrated by analyzing the XFROG spectrogram without relying on iterative calculations. A broad range of shapes can be analyzed from highly chirped pulses to short transients close to the bandwidth limit. The collinear excitation geometry is well suited for pulse analysis in multiphoton microscopes which are applied to biomedical imaging. The method may also find application in the characterization of single-cycle laser pulses [18]. The need for a gate pulse seems to be a drawback at first sight but pulse replicas from ultrashort laser sources which are typically present in multiphoton microscope laboratories can be used for its generation.

#### Acknowledgments

Financial support from the Baden-Württemberg Stiftung is gratefully acknowledged.